Published in final edited form as:
Chem Biol. 2012 April 20; 19(4): 507–517. doi:10.1016/j.chembiol.2012.02.006.

Designing photoswitchable peptides using the AsLOV2 domain

Oana I. Lungu[1,2,3], **Ryan A. Hallett**[1], **Eun Jung Choi**[1], **Mary J. Aiken**[1], **Klaus M. Hahn**[2,3], and **Brian Kuhlman**[1]

[1]Department of Biochemistry and Biophysics, University of North Carolina, Chapel Hill, North Carolina 27599, USA

[2]Department of Pharmacology, University of North Carolina, Chapel Hill, North Carolina 27599, USA

[3]Lineberger Comprehensive Cancer Center, University of North Carolina, Chapel Hill, North Carolina 27599, USA

Summary

Photocontrol of functional peptides is a powerful tool for spatial and temporal control of cell signaling events. We show that the genetically encoded light-sensitive LOV2 domain of *Avena Sativa* phototropin 1 (AsLOV2) can be used to reversibly photomodulate the affinity of peptides for their binding partners. Sequence analysis and molecular modeling were used to embed two peptides into the Ja helix of the AsLOV2 domain while maintaining AsLOV2 structure in the dark, but allowing for binding to effector proteins when the Jα helix unfolds in the light. Caged versions of the ipaA and SsrA peptides, LOV-ipaA and LOV-SsrA, bind their targets with 49-fold and 8-fold enhanced affinity in the light, respectively. These switches can be used as general tools for light dependent co-localization, which we demonstrate with photoactivable gene transcription in yeast.

Introduction

Peptides regulate a variety of biological processes by acting as competitive inhibitors (Singh, et al., 2005), allosteric regulators (Lockless and Ranganathan, 1999) and localization signals (Conti, et al., 1998). Photocontrol of peptide activity is a powerful tool for precise spatial and temporal control of cellular function (Gautier, et al., 2010; Nguyen, et al., 2004). Typically, photoactivation of peptides has been achieved by covalently modifying peptides with chemical groups that inhibit function until they are removed by light (Moglich and Moffat, 2010; Young and Deiters, 2007). Because such derivatized peptides must usually be synthesized *in vitro*, one challenge of this approach is getting the peptides into living cells or animals. Additionally, in most cases the photoinduced reaction is not reversible. Recently, there has been considerable progress in the use of naturally occurring photoactivable proteins to engineer light switches that are genetically encoded and reversible (Kennedy, et al., 2010; Levskaya, et al., 2009; Wu, et al., 2009; Yazawa, et al., 2009). In the majority of

*Co-corresponding authors: Klaus M. Hahn: 919.843.2775, klaus_hahn@med.unc.edu; Brian Kuhlman: 919.843.0188 bkuhlman@email.unc.edu.
Contact information: Oana I. Lungu: oilungu@gmail.com; **Ryan A. Hallett:** rhallett19@gmail.com; **Eun-Jung Choi:** s_banshe@yahoo.com; **Mary J. Aiken:** JetAiken@unc.edu

cases, the goal has been to regulate the activity of folded protein domains. Here, we examine if the LOV2 domain from *Avena sativa* phototropin 1 (AsLOV2) can be used to photomodulate the affinity of peptides for binding partners (Huala, et al., 1997).

AsLOV2 is part of the PAS superfamily of domains (Crosson and Moffat, 2001). It contains a flavin mononucleotide (FMN) co-factor located in the center of the PAS fold, as well as a large α-helical region C-terminal to the fold, termed the Jα helix (Halavaty and Moffat, 2007; Harper, et al., 2003). Upon irradiation with blue light, a covalent adduct is formed between a cysteine side chain in the PAS fold and a carbon atom of the FMN (Crosson and Moffat, 2002; Swartz, et al., 2001). Spectroscopy studies indicate this leads to a large conformational change in the domain, including the unfolding of the Jα helix (Harper, et al., 2004; Swartz, et al., 2002). When irradiation ceases, reversion of the thiol bond and conformational change back into the dark state occurs spontaneously within seconds to hours, depending on the LOV domain ortholog (Zoltowski, et al., 2009).

The large conformation change that occurs within the Jα helix has been previously harnessed to create a photoswitchable GTPase, PA-Rac (Wu, et al., 2009); a photoswitchable variant of *E. coli* trp repressor that has enhanced affinity for DNA in the light, LOV-TAP (Strickland, et al., 2008; Strickland, et al., 2010); and a photoactivatable DHFR enzyme (Lee, et al., 2008). In these studies, entire protein domains were fused to the end of the Jα helix in order to sterically occlude binding with effector molecules or perturb the conformational state of the attached domain. Upon blue light irradiation, unfolding of the Jα helix relieves the steric block or conformational strain.

Because peptides are more flexible than folded domains, it may not be sufficient to place them at the end of the Jα helix to achieve a steric block; tighter caging may be obtained by embedding their functionality within the Jα helix (Figure 1). A similar strategy has been successful for caging coiled-coil peptides in the light-sensitive photoactive yellow protein (PYP)(Fan, et al., 2011). In the case of AsLOV2, the challenge is identifying sequences that incorporate the target binding of the peptide while maintaining the functionality of the Jα helix. One face of the Jα helix is exposed to solvent while the other face forms hydrophobic interactions with a β-sheet in the AsLOV2 domain. Residues on the surface of the helix are expected to be tolerant to mutation, while the buried residues should be more conserved. Similarly, most peptides have sets of residues that are required for binding target proteins, while other positions can be varied. These observations indicate that it may be possible to identify chimeric sequences for the Jα helix that maintain key interactions with the AsLOV2 domain but incorporate residues critical to peptide function. In this study, we use sequence comparisons along with molecular modeling to create AsLOV2 variants that embed the binding properties of the ipaA (Van Nhieu, et al., 1997) and SsrA (Levchenko, et al., 2003) peptides in the Jα helix.

The usefulness of a photoswitch depends on how much the activity is enhanced by light irradiation (dynamic range) as well as the absolute activity in the dark and in the light. Naturally occurring protein switches vary considerably with regard to absolute activities and dynamic range, indicating that the appropriate switching power for a particular application is likely to be system dependent. For instance, the AsLOV2 derived PA-Rac switch binds to its effector with an affinity of 2 μM in the dark and 200 nM in the light (Wu, et al., 2009), which is appropriate for modulating cellular signaling because a similar change in binding affinity occurs when Rac1 naturally cycles between the GDP and GTP bound state (Thompson, et al., 1998). Studies with the wild type AsLOV2 domain indicate that it should be possible to create AsLOV2-based switches that show larger changes in activity upon light activation. NMR studies have shown that light activation changes the ratio of docked to undocked Jα helix from 98.4:1.6 in the dark to 9:91 in the lit state (Yao, et al., 2008). This

corresponds to a 3.8 kcal mol^{-1} change in free energy which if efficiently harnessed could be used to create switches that have greater than one hundred-fold changes in binding affinity for target molecules. In scenarios that involve competitive binding to the Jα helix, i.e. the helix is either docked against the LOV domain or bound to an effector molecule, it may be necessary to stabilize the helix docked state in order to take full advantage of the free energy perturbation that light activation provides. Strickland et al. showed that mutations that stabilize the docked Jα helix could be used to lower the dark state affinity of LOV-TAP for DNA and improve its dynamic range from 5-fold to 70-fold (Strickland, et al., 2010). Here, we identify further mutations that stabilize a docked Jα helix and show that the peptide switches can also be tuned by varying the location where the caged sequence is embedded in the Jα helix and by varying the intrinsic affinity of the peptide for its target.

As an application of our tunable peptide photoswitches, we show that the caged ipaA peptide can be used to induce transcription through light-activated heterodimerization in yeast, demonstrating that the caged peptides can be used as general tools for co-localizing proteins in living cells.

Results

Identifying Peptides Compatible with AsLOV2 Caging

To identify protein-binding peptides well suited for caging with the AsLOV2 domain we searched the protein database (PDB) for peptide sequences similar to portions of the Jα helix. The similarity score for each position in the alignment was weighted based on how likely a match or mismatch was to disrupt caging or peptide binding. For instance, if a position in the alignment mapped to residues important for both the AsLOV2-Jα helix interaction and the peptide-protein interaction, then a large favorable score was given if the amino acids were identical, and a large unfavorable score was given if the amino acids were dissimilar. The importance of a residue to the AsLOV2-Jα helix interaction or the peptide-protein interaction was assigned based on how buried the residue was; residues that were more buried were considered more important. There was little reward or penalty for conserving amino acids on the surface of the Jα helix. Using a sliding window of 6 residues, the sequence of the Jα helix was aligned with over 3000 peptide sequences taken from crystal structures of peptides co-crytallized with their protein-binding partners. Peptides from several hundred structures were identified as candidates for caging with the AsLOV2 domain. It is worth noting that this approach can be expanded to also consider known protein-binding peptides that have not been crystallized with their binding partners.

We picked out two peptide sequences for experimental testing and optimization: a vinculin binding peptide from the invasin protein ipaA (Izard, et al., 2006) and the SsrA peptide from *E. Coli*, which binds the protease delivery protein SspB (Levchenko, et al., 2003). These sequences were chosen for a variety of reasons. First, at functionally important residues they align well with the Jα helix (Figure 2A,B). Indeed, several alternative alignments were identified for the SsrA peptide. Second, they adopt alternative conformations when binding their targets, ipaA adopts a helix while SsrA binds in an extended conformation (Figure S1). By testing both peptides, we examine if our approach can be used to cage peptides regardless of the conformation they adopt when bound to their target protein. Third, the peptides have different intrinsic affinities for their target proteins. IpaA binds the D1 domain of vinculin very tightly, $K_d < 1$ nM, while SrrA binds SspB with an affinity of ~30 nM.

Finally they have complementary advantages for use in controlling cell biology. The SsrA and SspB sequences are specific to bacteria, and therefore it is expected that they will not interact with other proteins and peptides in higher organisms. Fusing proteins of interest to a photoactivable SsrA and SspB should provide a general approach for light-induced

heterodimerization, which can be used to localize proteins in the cell and activate cell-signaling pathways. Vinculin and ipaA-like peptides are found in mammals, and therefore caged ipaA should only be useful as a general tool for co-localization in orthogonal systems such as yeast. However, caged ipaA may be useful for probing vinculin biology in mammalian cells. Vinculin is a protein that connects integrin binding proteins such as talin (Cohen, et al., 2006) to the actin cytoskeleton at focal adhesions (Saunders, et al., 2006) and adherens junctions (Carisey and Ballestrem, 2010), cellular structures important for determining cell shape and motility. The ipaA peptide is from the IpaA protein of the *Shigella flexneri* bacterium, and binds to the talin binding site on vinculin (Izard, et al., 2006). It has been proposed that IpaA binding prevents vinculin from binding talin, and thus linking integrin signaling to the actin cytoskeleton. Selectively photo-controlling the binding of ipaA to vinculin through the LOV-ipaA photoswitch could render it useful as a dominant negative inhibitor of vinculin in mammalian cells, and an integral tool for studying the role of vinculin dynamics in cell motility.

Design of LOV-ipaA

In our search of peptides in the protein database, the first ten residues of the ipaA VBS1 helical peptide were identified as a close match to the last ten residues of the AsLOV2 Jα helix (Figure 2A). Five of the ten positions are identical, and the hydrophobic residues on the Jα helix that make critical contacts with the AsLOV2 domain β-sheet at residues 539 542, and 543 are conserved in the alignment with ipaA. Additionally, residues in the ipaA sequence that make extensive contacts with vinculin are conserved in the alignment (Ile 612, Ala 615, Ala 616, and Val 619 in ipaA). This analysis suggests that it should be possible to design a chimeric sequence for the Jα helix that is compatible with the AsLOV2 structure and will bind vinculin when undocked from the AsLOV2 structure.

To design the chimeric sequence the Rosetta molecular modeling program was used to assess the impact of altering the AsLOV2-Jα and vinculin-ipaA complex sequences (Das and Baker, 2008). Side chain optimization simulations were used to thread the first ten residues of ipaA onto the last ten residues of the Jα helix. The Rosetta scores of individual residues were examined to determine if particular residues in the ipaA sequence packed unfavorably against the AsLOV2 domain β-sheet. A single position showed unfavorable scores, the mutation of aspartic acid 540 to tyrosine. To search for an alternative amino acid to place at this position, Rosetta was used to perform a sequence optimization simulation in which position 540 was allowed to adopt alternative identities and neighboring side chains were free to adopt new side chain conformations. One of the best scoring residues in the 540 position on the Jα helix was isoleucine. A working model for LOV-ipaA was then created by using the threaded AsLOV2-Jα design and adding the remaining 11 residues of ipaA onto the C-terminal end of Jα using the fragment insertion capability of Rosetta's domain assembly protocol (Figure 2C).

Dark and Lit state binding between LOV-ipaA and vinculinD1

We developed a fluorescence polarization competition assay to measure the binding affinity and kinetics of LOV-ipaA to the vinculinD1 subdomain under dark as well as blue light irradiation conditions (Figure 3A). LOV-ipaA was titrated into a mixture of the vinculinD1 subdomain bound to ipaA peptide labeled with the dye 5-(and-6)-Carboxytetramethylrhodamine (TAMRA). As LOV-ipaA bound to vinculin the dye-labeled peptide was competed off and its fluorescence polarization signal decreased. Initial experiments showed that the slow intrinsic off-rate of the ipaA peptide and LOV-ipaA from vinculin made it possible to monitor both the kinetics and thermodynamics of binding over a time course of several hours. Experiments with varying amounts of LOV-ipaA were fit

simultaneously for the on rate and binding affinity of LOV-ipaA to vinculinD1 in Matlab using a numerical integration protocol.

The same concentrations of LOV-ipaA under either blue light irradiation or dark state conditions yielded different kinetic curves (Figure 3B,C). The binding affinity of LOV-ipaA WT in the light is 3.5 nM, while it is 69 nM in the dark, a 19-fold change (Table 1). The change in binding affinity upon light activation is primarily due to changes in the on rate for binding, in the dark the rate constant is 1.3×10^{3} M^{-1} s^{-1} and in the light it is 1.4×10^{4} M^{-1} s^{-1}. Similar changes were observed for LOV-ipaA mutants that abolish FMN-thiol bond formation (C450A) and lead to a pseudo dark state or mutants that destabilized the Jα helix (A532E I536E), causing a pseudo lit state conformation. These results are consistent with the proposed mechanism of caging. In the dark, the Jα helix is primarily docked against the AsLOV2 domain and the peptide is presented less frequently to the target binding site, slowing the on rate for binding. In general, the on rates for binding are slow both in the lit and dark state. Peptides and proteins often have k_{on} values greater than 1×10^{5} M^{-1} s^{-1} (Alsallaq and Zhou, 2008). The slow rates observed here are consistent with the helix addition mechanism of ipaA binding to vinculin, wherein the vinculin D1 4-helix bundle is rearranged into a 5-helix bundle through the addition of ipaA (Tran Van Nhieu and Izard, 2007).

Optimization of LOV-ipaA—We tested two sets of mutations predicted to enhance the dynamic range of the LOV-ipaA photoswitch. The first set of mutations were designed by Strickland *et al.* (Strickland, et al., 2010) to stabilize the helical structure of Jα. The mutations, G528A and N538E, increased the dynamic range of the LOV-TAP photoswitch for its effector from 5-fold to 70-fold. When used in the LOV-ipaA system, the mutations did have a large effect on LOV-ipaA dark state binding to vinculinD1, decreasing affinity more than 7-fold to 475 nM (Table 1). However, the mutations also weakened lit state binding affinity over 10-fold, to 110 nM. The net effect of the G528A and N538E mutations in LOV-ipaA then, was a decrease in the photoswitching dynamic range of the protein. The weakened affinity for vinculin in the lit state is likely due to charge-charge repulsion between Glu538 in LOV-ipaA (G528A, N538E) and a glutamate close to the binding site of ipaA in vinculin.

We designed a second set of mutations to increase the dynamic range of the switch, L514K L531E, using the interactive modeling program FoldIt (Cooper, et al., 2010). These mutations replaced two hydrophobic residues, one in the Jα helix, and the other on the β-sheet contacting the Jα helix, with a salt bridge. The design was meant to stabilize interactions between the β-sheet and Jα helix and lead to a more tightly bound helix in the dark state. Indeed, the binding affinity of LOV-ipaA L514K L531E to vinculinD1 in the dark state weakened to 245 nM, while the lit state affinity increased only slightly, to 5 nM. This set of mutations make LOV-ipaA a photoswitch with a 49-fold difference between the lit state and dark state effector binding affinities.

To independently validate results from the florescence polarization competition assay, surface plasmon resonance experiments were also conducted. The on rate, off rate, and binding affinity of vinculinD1 to LOV-ipaA L514K L531E were measured. LOV-ipaA L514K L531E pseudo lit (A532E I536E) (Harper, et al., 2004) and pseudo dark (C450A) (Salomon, et al., 2000) states were used. Pseudo-dark state LOV-ipaA L514K L531E (Figure 3D) was able to bind vinculinD1 with an on rate of 4.5×10^{2} M^{-1} s^{-1} and an off rate of 2.9×10^{-5} s^{-1}. A binding affinity of 64 nM was calculated from the kinetic data. The on rate was identical to that measured for LOV-ipaA L514K L531E under dark state condition using the fluorescence polarization assay. The off rate varied slightly, leading to a 4-fold difference in binding affinity between the two measurements. In part, the discrepancy might

be due to the fact that it is difficult to fit an off rate that is so slow. Measuring the LOV-ipaA L514K L531E pseudo lit photoswitch binding to vinculinD1, an on rate of 3.8×10^4 M^{-1} s^{-1} and an off rate of 8.7×10^{-5} s^{-1} were obtained (Figure 3E). Fitting indicated that the binding affinity was 2.3 nM. These values are similar to the kinetic rates measured for the LOV-ipaA lit mimetic using the fluorescence polarization assay.

There is a 49-fold increase in binding affinity for vinculin when LOV-ipaA L514K L531E is activated with light, but binding in the dark is still considerable, 245 nM. For some applications, it may be useful to have a switch that has weaker binding affinity in the dark. To test if we could switch the range of affinities over which LOV-ipaA functions, we made a mutation to LOV-ipaA that was predicted to reduce affinity for vinculin, but should have negligible effect on the interactions between the Jα helix and the LOV domain. This mutant, L623A, weakened the affinity of the LOV-ipaA lit state mimetic for the vinculin D1 domain from 3 nM to 2.4 μM, while the dark state mimetic had no detectable binding as monitored with isothermal titration calorimetry, suggesting that binding in the dark is weaker than 40 μM (Figure S2).

Design and Optimization of LOV-SsrA

We extended the design strategy used to cage ipaA in order to create a second photoswitchable peptide, LOV-SsrA. The SsrA peptide interacts with the protease delivery protein SspB from *E. coli* as a linear epitope using the seven residue sequence AANDENY (Levchenko, et al., 2003). Three possible alignments between SsrA and the Jα helix were identified in our PDB-wide search, one towards the N-terminal side of the helix (LOV-SsrAN), one near the C-terminal end (LOV-SsrAC), and one in the middle of the helix (LOV-SsrAM) (Figure 2B). We first tested the C-terminal alignment, LOV-SsrAC.

In LOV-SsrAC, the two alanines from SsrA were aligned with A542 and A543 from the last helical turn of the Jα helix, and the final three residues of the Jα helix were replaced with residues from the SsrA binding sequence (Figure 2D). Except for the last leucine, all buried positions in the Jα helix are conserved with this alignment, which only embeds the peptide in a single helical turn of the Jα helix. In comparison, the ipaA peptide is embedded within two helical turns in LOV-ipaA. To measure the affinity of LOV-SsrA for SspB in the dark and light, a fluorescence polarization competition assay was performed with TAMRA-labeled SsrA peptide. Unlike ipaA, SsrA binds rapidly to SspB and only equilibrium populations could be measured. The initial LOV-SsrA design showed a two-fold change in affinity when activated with light, 31 nM to 57 nM (Table S1). As lit state binding was near native in affinity for SspB, approaches to stabilize the Jα helix and therefore decrease dark state affinity were explored. We tested mutations previously shown to stabilize the Jα helix, G528A and N538E, as well as extensions to the C-terminus of LOV-SsrAC. G528A and N538E had the desired effect and lowered dark state affinity to 570 nM with a 5-fold change upon light activation. Extensions of varying lengths were designed with Rosetta (Kleiger, et al., 2009) with the goal of binding the surface of the AsLOV2 domain, thereby constraining SsrA to a single, non-binding conformation. The target surface on AsLOV2 was a hydrophobic patch immediately adjacent to the C-terminus of the Jα helix. Two extensions were experimentally tested, the addition of a single phenylalanine and the addition of the sequence GYGNL. The longer extension had no detectable effect, while the single phenylalanine increased the dynamic range of the switch to 8-fold (Figure 4A).

The LOV-SsrAN designs incorporating the N-terminal alignment of SsrA, had similar dynamic ranges to their corresponding C-terminal alignments. However, all had drastically reduced affinity for SspB in both the lit and dark state, > 10 μM. The initial N-terminally aligned designs showed an approximate 2-fold increase in affinity after exposure to blue light. The addition of the G528A and N538E mutations slightly weakened the lit state

affinity for SspB to 12.6 μM and the dark state affinity to 49 μM (Figure 4B). Because of constraints imposed by the AsLOV2 domain, the SspB binding sequence used in LOV-SsrAN was AANDEAY instead of AANDENY as used in LOV-SsrAC. To determine if the sequence change was responsible for the lower dark and lit-state affinities for SspB, a peptide with the same sequence as LOV-SsrAN was synthesized and binding to SspB was measured. Binding was tight, 38 nM, suggesting that the reduced affinity for SspB was not because of changes to the binding sequence, but rather because of the location within the Jα helix that the peptide was embedded. Results with LOV-SsrAM were more ambiguous, as the sequence embedded in the Jα helix, AANDINY, showed reduced affinity for SspB as a peptide (1.9 μM). However, lit (40 μM) and dark state (156 μM) state affinities were still significantly lower than that the isolated peptide, suggesting again that embedding sequences deeper in the Jα helix lowers accessibility to the peptide in both the dark and light (Figure S3).

The reversibility of LOV-SsrA switches was tested by monitoring their ability to compete with a TAMRA-labeled SsraA peptide for binding to SspB over multiple rounds of irradiation followed by incubation in the dark (Figure 4C). As monitored indirectly from following the fluorescence polarization signal from the SsraA peptide, the fraction of LOV-SsrA molecules switching from the bound to unbound state remained unchanged over multiple rounds of illumination, indicating that the switches are reversible. To check that the observed results were not an artifact due to interaction between the blue light and the TAMRA dye, similar reversion experiments were performed with only SspB and labeled peptide. No polarization changes were observed after incubation with blue light. The reversibility experiments also showed that dark state equilibrium was reached within 15 seconds, quicker than what has) been observed previously for the AsLOV2 domain. Half-times between 27 and 50 seconds have been reported for the LOV2 domain from *Avena sativa* (Salomon, et al., 2000; Swartz, et al., 2001). Using absorption spectroscopy, we determined the half-life of LOV-SsrAC's photocycle to be 2.7 ± 0.4 seconds, with a similar relaxation time in the presence of saturating concentrations of SspB, 2.3 ± 0.1 seconds (Figure S3). At this point it is not clear why LOV-SsrAC has an unusually fast rate of reversion to the dark state, but this could be advantageous in applications where quick switching from the bound to unbound state is critical.

LOV-ipaA binding to Full-length Vinculin: Actin co-sedimentation assays

Having established the AsLOV2 domain could be used to cage peptides, we tested if LOV-ipaA could be used to perturb vinculin in a biologically relevant manner. Actin co-sedimentation assays were performed to measure the apparent binding affinity of LOV-ipaA to full-length vinculin. Vinculin naturally forms an autoinhibited conformation stabilized by interactions between the head domain (including the D1 domain) and tail domain. Binding of the ipaA peptide to the head domain competes with the autoinhibited state and releases the tail domain to bind with polymerized F-actin (Izard, et al., 2006). Actin co-sedimentation assays were performed to measure the apparent binding affinity of LOV-ipaA in the dark and lit state to full-length vinculin. In the assay, polymerized actin, vinculin, and LOV-ipaA (lit or dark-state mutants) were incubated together (Figure 5A). Only vinculin that bound to LOV-ipaA should be able to interact and bind to F-actin. The resulting mix of bound and unbound vinculin was centrifuged at high speeds, resulting in fractionation of F-actin polymers out of solution, along with the vinculin-LOV-ipaA complexes that had bound to them. An SDS-page gel was used to monitor the amount of vinculin that fractionated out of solution along with F-actin as a function of the total concentration of vinculin, thereby determining the fraction of full-length vinculin bound to LOV-ipaA. The assay was repeated at several concentrations of LOV-ipaA to create a binding curve and calculate apparent binding affinities (Figure 5B and C). In general, the affinities are expected to be

considerably weaker with full-length vinculin than those observed for binding to the isolated D1 domain, because in the full-length protein there is competition with the autoinhibited state of vinculin (Le Clainche, et al., 2010). For instance, peptides from the protein talin bind to the vinculin D1 domain with an affinity of 15 nM, but bind to full-length vinculin with an affinity of ~5 μM (Izard and Vonrhein, 2004; Le Clainche, et al., 2010). LOV-ipaA with the lit state mutant bound with an apparent affinity of 8 μM to vinculin, while the dark state mimetics bound with an affinity of 56 μM (Table S2). The binding of vinculin to ipaA in the presence of polymerized actin also gives us a window into the reactions that occur *in vivo*, where full-length vinculin must be bound both by talin and by F-actin in order to engage in integrin signaling. The difference in binding affinity between lit and dark states of LOV-ipaA to full-length vinculin in the presence of polymerized actin suggests that LOV-ipaA may be a relevant photoswitch for probing such signaling *in vivo*.

Photoactivatable yeast transcription

To demonstrate that the caged peptides can be used to co-localize proteins and activate signaling events in living cells, we used the LOV-ipaA-vinculinD1 interaction as a heterodimerization switch for controlling gene transcription. The experiments were performed in S. cerevisiae, as it is an orthogonal system, lacking proteins that would cross-react with the LOV-ipaA-vinculinD1 interaction. We linked LOV-ipaA L623A to the GAL4 activation domain (AD), while linking vinculinD1 (vinD1) to the GAL4 binding domain (BD), and monitored the GAL4-induced activation of the transcriptional GAL promoter through a yeast two-hybrid assay. This is a strategy that has been widely used to identify protein-protein interactions. In our case, LOV-ipaA and vinculinD1 should only interact upon irradiation with blue light, thus bringing the GAL4 AD and BD into proximity (Figure 6A). The full GAL4 protein can then activate the expression of reporter genes downstream of the GAL promoter. We tested the ability to activate the reporter gene LacZ under both dark state and lit state conditions through quantification of β-galactosidase activity (Figure 6B). We observed an activity of 5 Miller Units under blue light conditions, and an activity of 20 Miller Units with the LOV-ipaA L623A lit state mimetic and 30 units using the ipaA peptide. Almost no activity (0.4 Miller Units) was seen under dark or dark state conditions, and no activity was seen in empty vector negative controls. We also tested activation of genes MEL1, HIS3, and ADE2 under dark and lit state conditions by replica plating BD-vindD1 colonies mated with AD-LOV-ipaA L623A lit state and dark state mimetic mutants or AD-LOV-ipaA L623A WT (Figure 6C). We saw strong growth of colonies containing LOV-ipaA L623A lit mimetic or WT grown in blue light on plates lacking His as well as those lacking His and Ade, indicating expression of both HIS3 and ADE2 genes. Furthermore, colonies were blue, indicating expression of the MEL1 gene whose product, α-galactosidase, interacted with the x-α-gal substrate for blue screening. Colonies containing LOV-ipaA L623A dark mimetic or WT grown in the dark grew on control plates, but did not grow on plates lacking His or Ade, showing low to no expression of HIS2, ADE2 or MEL1 genes. This indicates that LOV-ipaA-vinculinD1 heterodimerization can be used as a tool to photocontrol yeast gene expression.

The LOV-ipaA L623A mutation was critical to achieving a lit state to dark state change of phenotype in yeast gene expression. When experiments for MEL1 and HIS3 were conducted using LOV-ipaA lacking this mutation, no observable growth change was seen between colonies containing lit state and dark state AD-LOV-ipaA mated with BD-vinD1 (Figure S4). The binding affinity of LOV-ipaA to vinculinD1, was hence, so tight, even in the dark state, as to allow binding events and subsequently yeast gene expression to occur. The L623A mutation shifted the binding affinity of LOV-ipaA for vinculinD1 to a range where there was no binding in the dark, but significant activation in the light. This result highlights the usefulness of being able to tune the switches for specific applications.

Discussion

We have shown that protein-binding peptides can be embedded in the AsLOV2-Jα helix so that their affinity for effector proteins is weakened in the dark, but is enhanced when light-activation releases the Jα helix from the LOV domain. The approach is applicable to a variety of peptide sequences because only a subset of residues on the Jα helix need to be conserved to maintain favorable interactions with LOV domain. Additionally, most protein-binding peptides contain residues that can be mutated without significantly weakening affinity for binding partners. In the case of LOV-ipaA and LOV-SsrAC we also took advantage of the fact that not all of the peptide needs to be embedded in the Jα helix to create a steric block against effector binding. In this scenario, only a few residues from the N-terminal portion of the peptide need to be compatible with the folded Jα helix.

For some applications it may be necessary to tune the designed photoswitch to have a dark state activity and dynamic range compatible with the desired outcome. In the yeast two-hybrid experiments with LOV-IpaA we found that we needed to weaken dark state binding in order to prevent gene expression in the dark. We accomplished this by introducing a mutation that weakens the baseline affinity of IpaA for vinculin. While the initial design switched from 3.5 nM to 69 nM affinity for vinculin, the mutant switched from 2.4 μM to >40 μM. The switching power of the LOV-peptide switches were also manipulated by introducing mutations that stabilize the interaction between the Jα helix and the rest of the LOV domain, as well as by varying how deeply the caged peptide was embedded in the helix. It was somewhat surprising that the SsrA peptide had significantly lower lit state affinity for SspB when embedded in the N-terminal portion of the Jα helix than when placed at the C-terminus. NMR experiments with the WT AsLOV2 domain indicate that the helix undocks as a cooperative unit when the protein is activated with light (Yao, et al., 2008). This suggests that there should be similar levels of access to residues in the N-terminal and C-terminal regions of the Jα helix in the lit state, and therefore, we expected that lit-state binding affinity for the peptide would be relatively insensitive to where the peptide was placed in the Jα helix. Our results indicate that the N-terminal portion of the Jα helix may be less accessible in the lit state, perhaps by transient interactions with the hydrophobic face of the LOV domain β sheet. Additionally or alternatively, the mutations we have made to the Jα helix to create LOV-SsrAN may have resulted in stronger interactions between the Jα helix and the rest of the AsLOV2 domain in the light.

Both the LOV-ipaA- vinculinD1 and the LOV-SsrA-SspB photoactivatable binding interactions can be harnessed as tools for photoactivatable heterodimerization. The LOV-ipaA- vinculin switch can be used in bacteria and in yeast cells, as these systems do not contain vinculin or vinculin binders that would affect the LOV-ipaA-vinculin interaction. The LOV-SsrA-SspB photoactivatable heterodimerization binders, on the other hand, should be useful in higher organisms such as mammalian cells. LOV-ipaA has a very slow off rate for vinculinD1, so it is better suited for long time-scale applications such as yeast mating. In contrast, LOV-SsrA binding to SspB is rapidly reversible so can be used for more transient interactions, such as single cell motility experiments. In these ways, both LOV-ipaA and LOV-SsrA should be useful tools to spatially and temporally bring together proteins for activating signaling cascades.

Significance

Peptides regulate a variety of biological processes by acting as competitive inhibitors, allosteric regulators, and localization signals. Photocontrol of peptide activity is a powerful tool for precise spatial and temporal control of cellular function. Our work in this paper focuses on designing and characterizing peptides caged by embedding their sequences into the Jα helix of the AsLOV2 domain. The peptides ipaA and SsrA were both effectively

caged in this manner, allowing for enhanced peptide-effector binding in the light. Mutations introduced into the AsLOV2 domain increased the difference between lit state and dark state effector binding, while the position where the caged sequence is embedded in the Jα helix and the intrinsic affinity of the peptide for its target tunes the range of affinities of the photoactivatable peptide . We discuss ways in which other peptides may be caged in a similar manner using the AsLOV2 domain. We also apply LOV-ipaA as a tool for photoactivatable gene transcription in *S. cerevisiae*, and describe potential uses for LOV-SsrA.

Experimental Procedures

Cloning

The LOV-ipaA gene was synthesized with a 6 histidine N-terminal tag (Genscript) and cloned into the pET21b vector. The genes for LOV-SsrA and monomeric SspB were synthesized (Genscript) and cloned into pQE-80L and pTriEX4 vectors respectively. All mutations were performed using site-directed mutagenesis. The VinculinD1 subdomain (residues 1-258) and full-length vinculin (residues 1-1066) were cloned into a pET15b vector. See Supplementary Methods for protein expression and purification.

Peptides

Peptides containing the sequence TANNIIKAAKDATTSLSKVLKNIN, TANNIIKAAKDATTSASKVLNIN, TANNIIKAAKDATTSLSKALKNIN, QIEEAANDENY , LIKKAANDINYAAK, and HVRDAANDEAYMLIK were synthesized at UNC-Chapel Hill and amine labeled using 5-(and-6)-Carboxytetramethylrhodamine (TAMRA) dye (Anaspec). Peptide concentration was determined by measuring absorbance of the TAMRA dye at 555 nm using 65,000 M^{-1} cm^{-1} extinction coefficient.

Fluorescence polarization experiments

All fluorescence polarization experiments were conducted using a Jobin Yvon Horiba FluoroMax3 fluorescence spectrometer. TAMRA labeled peptides were excited with polarized light at 555 nm and the polarization of emitted light was measured at 583 nm. See Supplementary Methods for detailed methods.

Surface Plasmon Resonance

Surface plasmon resonance experiments were conducted using a Biacore 2000 machine (GE). VinculinD1 was immobilized through amine coupling to the surface of a CM5 chip (GE) Different concentrations of LOV-ipaA mutants were flown over the immobilized protein and the change in response units over time was recorded. Data were fit simultaneously for k_{on} and k_{off} to a pseudo-first order binding model.

Actin co-sedimentation assays

Purified rabbit actin (invitrogen) was polymerized for 30 min at room temperature in 10 mM Tris-HCl pH 7.5 containing 100 mM KCl, 2 mM MgCl2 , 2 mM DTT and 1 mM ATP. 2 uM vinculin and either ipaA peptide or LOV-ipaA mutants were mixed for vinculin:ipaA rations of 1:0, 1:1, 1:2.5, 1:5, 1:10, 1:20, or 1:50 per sample. 12 μM polymerized actin was added per sample, within a volume of 45 μL per sample. Samples were incubated at room temperature for 1 hour. They were then centrifuged in a TLA-100 rotor in a Beckman Coulter Optimax XP ultracentrifuge at an acceleration of 150,000 g for 30 min cooled to 20°C. Samples were split into supernatant and pellet fractions. Pellets were re-suspended into 45 μL 2x tris-glycine SDS buffer. All fractions were denatured and run onto an 8% SDS-page polyacrylamide gel. Gels were coomassie stained and analyzed using ImageJ

software to determine the fraction of vinculin present in the pellet versus total vinculin in each sample (Le Clainche, et al., 2010).

Yeast two hybrid assays

LOV-ipaA L623A WT, lit state mutants, dark state mutants, and ipaA were cloned into a pGADT7 vector and transformed into *S. cerevisiae* Y187 strain, while the vinculinD1 subdomain was cloned into a pGBKT7 vector and transformed into *S. cerevisiae* Y2Hgold strain (Clontech). Empty vectors were also transformed into the appropriate strains. Transformed colonies of Y2Hgold and Y187 were mated at 30°C overnight and plated on synthetic dextrose (SD) -Leu -Trp media. For yeast two-hybrid experiments, mated colonies were serially diluted (1:5, from right to left on plates shown) and replica plated onto SD–Leu–Trp media; SD–Leu–Trp media with auerobasidin A and 5-bromo-4-chloro-3-indolyl-α-D-gactopyranoside (x-α-gal); SD–Leu–Trp–His media with auerobasidin A and x-α-gal; and SD–Leu–Trp–His–Ade media with auerobasidin A and x-α-gal. Plates were grown for 3 days at 30°C. For Miller assays, mated colonies were picked and grown to saturation in SD–Leu–Trp media. Saturated colonies were diluted to low-log phase and grown for 4 hours under dark or blue light conditions. Cells were lysed open and treated with Chlorophenol red-β-D-galactopyranoside (CPRG, Roche) substrate to determine β-galactosidase activity in Miller Units (Kennedy, et al., 2010).

Supplementary Material

Refer to Web version on PubMed Central for supplementary material.

Acknowledgments

We thank A. Tripathy and the Macromoleular Interaction core facility at UNC-Chapel Hill for help in biophysical experiments, C. A. Purbeck for help and advice in conducting yeast 2-hybrid experiments, and M. Rougie for help with vinculin studies. This work was supported by grants from the NIH (GM093208 and GM057464) and the American Heart Association (09PRE2100055) (To O.I.L).

References

Alsallaq R, Zhou H-X. Electrostatic rate enhancement and transient complex of protein–protein association. Proteins. 2008; 71:320–335. [PubMed: 17932929]

Carisey A, Ballestrem C. Vinculin, an adapter protein in control of cell adhesion signalling. Eur. J. Cell Biol. 2010; 90:157–163. [PubMed: 20655620]

Cohen DM, Kutscher B, Chen H, Murphy DB, Craig SW. A Conformational Switch in Vinculin Drives Formation and Dynamics of a Talin-Vinculin Complex at Focal Adhesions. J. Biol. Chem. 2006; 281:16006–16015. [PubMed: 16608855]

Conti E, Uy M, Leighton L, Blobel G, Kuriyan J. Crystallographic Analysis of the Recognition of a Nuclear Localization Signal by the Nuclear Import Factor Karyopherin α. Cell. 1998; 94:193–204. [PubMed: 9695948]

Cooper S, Khatib F, Treuille A, Barbero J, Lee J, Beenen M, Leaver-Fay A, Baker D, Popovic Z, players F. Predicting protein structures with a multiplayer online game. Nature. 2010; 466:756–760. [PubMed: 20686574]

Crosson S, Moffat K. Photoexcited structure of a plant photoreceptor domain reveals a light-driven molecular switch. Plant Cell. 2002; 14:1067–1075. [PubMed: 12034897]

Crosson S, Moffat K. Structure of a flavin-binding plant photoreceptor domain: insights into light-mediated signal transduction. Proc. Natl. Acad. Sci. USA. 2001; 98:2995–3000. [PubMed: 11248020]

Das R, Baker D. Macromolecular Modeling with Rosetta. Annu. Rev. of Biochem. 2008; 77:363–382. [PubMed: 18410248]

Fan HY, Morgan S-A, Brechun KE, Chen Y-Y, Jaikaran ASI, Woolley GA. Improving a Designed Photocontrolled DNA-Binding Protein. Biochemistry. 2011; 50:1226–1237. [PubMed: 21214273]

Gautier A, Nguyen DP, Lusic H, An W, Deiters A, Chin JW. Genetically Encoded Photocontrol of Protein Localization in Mammalian Cells. J. Am. Chem. Soc. 2010; 132:4086–4088. [PubMed: 20218600]

Halavaty AS, Moffat K. N- and C-terminal flanking regions modulate light-induced signal transduction in the LOV2 domain of the blue light sensor phototropin 1 from Avena sativa. Biochemistry. 2007; 46:14001–14009. [PubMed: 18001137]

Harper SM, Christie JM, Gardner KH. Disruption of the LOV-Jalpha helix interaction activates phototropin kinase activity. Biochemistry. 2004; 43:16184–16192. [PubMed: 15610012]

Harper SM, Neil LC, Day IJ, Hore PJ, Gardner KH. Conformational changes in a photosensory LOV domain monitored by time-resolved NMR spectroscopy. J. Am.Chem. Soc. 2004; 126:3390–3391. [PubMed: 15025443]

Harper SM, Neil LC, Gardner KH. Structural basis of a phototropin light switch. Science. 2003; 301:1541–1544. [PubMed: 12970567]

Huala E, Oeller PW, Liscum E, Han IS, Larsen E, Briggs WR. Arabidopsis NPH1: a protein kinase with a putative redox-sensing domain. Science. 1997; 278:2120–2123. [PubMed: 9405347]

Izard T, Tran Van Nhieu G, Bois PR. Shigella applies molecular mimicry to subvert vinculin and invade host cells. J. Cell Biol. 2006; 175:465–475. [PubMed: 17088427]

Izard T, Vonrhein C. Structural basis for amplifying vinculin activation by talin. J.Biol. Chem. 2004; 279:27667–27678. [PubMed: 15070891]

Kennedy MJ, Hughes RM, Peteya LA, Schwartz JW, Ehlers MD, Tucker CL. Rapid blue-light-mediated induction of protein interactions in living cells. Nat. Meth. 2010; 7:973–975.

Kleiger G, Saha A, Lewis S, Kuhlman B, Deshaies RJ. Rapid E2-E3 Assembly and Disassembly Enable Processive Ubiquitylation of Cullin-RING Ubiquitin Ligase Substrates. Cell. 2009; 139:957–968. [PubMed: 19945379]

Le Clainche C, Dwivedi SP, Didry D, Carlier M-F. Vinculin is a dually regulated actin filament barbed-end capping and side-binding protein. J. Biol. Chem. 2010; 189:1075–1077.

Lee J, Natarajan M, Nashine VC, Socolich M, Vo T, Russ WP, Benkovic SJ, Ranganathan R. Surface Sites for Engineering Allosteric Control in Proteins. Science. 2008; 322:438–442. [PubMed: 18927392]

Levchenko I, Grant RA, Wah DA, Sauer RT, Baker TA. Structure of a Delivery Protein for an AAA+ Protease in Complex with a Peptide Degradation Tag. Mol. Cell. 2003; 12:365–372. [PubMed: 14536076]

Levskaya A, Weiner OD, Lim WA, Voigt CA. Spatiotemporal control of cell signalling using a light-switchable protein interaction. Nature. 2009; 461:997–1001. [PubMed: 19749742]

Lockless SW, Ranganathan R. Evolutionarily Conserved Pathways of Energetic Connectivity in Protein Families. Science. 1999; 286:295–299. [PubMed: 10514373]

Moglich A, Moffat K. Engineered photoreceptors as novel optogenetic tools. Photochem. Photobiol. Sci. 2010; 9:1286–1300. [PubMed: 20835487]

Nguyen A, Rothman DM, Stehn J, Imperiali B, Yaffe MB. Caged phosphopeptides reveal a temporal role for 14-3-3 in G1 arrest and S-phase checkpoint function. Nat. Biotechnol. 2004; 22:993–1000. [PubMed: 15273693]

Nikolovska-Coleska Z, Wang R, Fang X, Pan H, Tomita Y, Li P, Roller PP, Krajewski K, Saito NG, Stuckey JA, et al. Development and optimization of a binding assay for the XIAP BIR3 domain using fluorescence polarization. Anal. Biochem. 2004; 332:261–273. [PubMed: 15325294]

Salomon M, Christie JM, Knieb E, Lempert U, Briggs WR. Photochemical and mutational analysis of the FMN-binding domains of the plant blue light receptor, phototropin. Biochemistry. 2000; 39:9401–9410. [PubMed: 10924135]

Saunders RM, Holt MR, Jennings L, Sutton DH, Barsukov IL, Bobkov A, Liddington RC, Adamson EA, Dunn GA, Critchley DR. Role of vinculin in regulating focal adhesion turnover. Eur. J. Cell Biol. 2006; 85:487–500. [PubMed: 16584805]

Singh N, Jabeen T, Sharma S, Roy I, Gupta MN, Bilgrami S, Somvanshi RK, Dey S, Perbandt M, Betzel C, et al. Detection of native peptides as potent inhibitors of enzymes. FEBS Journal. 2005; 272:562–572. [PubMed: 15654893]

Strickland D, Moffat K, Sosnick TR. Light-activated DN A binding in a designed allosteric protein. Proc. Natl. Acad. Sci. USA. 2008; 105:10709–10714. [PubMed: 18667691]

Strickland D, Yao X, Gawlak G, Rosen MK, Gardner KH, Sosnick TR. Rationally improving LOV domain-based photoswitches. Nat. Meth. 2010; 7:623–626.

Swartz TE, Corchnoy SB, Christie JM, Lewis JW, Szundi I, Briggs WR, Bogomolni RA. The photocycle of a flavin-binding domain of the blue light photoreceptor phototropin. J. Biol. Chem. 2001; 276:36493–36500. [PubMed: 11443119]

Swartz TE, Wenzel PJ, Corchnoy SB, Briggs WR, Bogomolni RA. Vibration spectroscopy reveals light-induced chromophore and protein structural changes in the LOV2 domain of the plant blue-light receptor phototropin 1. Biochemistry. 2002; 41:7183–7189. [PubMed: 12044148]

Thompson G, Owen D, Chalk PA, Lowe PN. Delineation of the Cdc42/Rac-binding domain of p21-activated kinase. Biochemistry. 1998; 37:7885–7891. [PubMed: 9601050]

Tran Van Nhieu G, Izard T. Vinculin binding in its closed conformation by a helix addition mechanism. EMBO J. 2007; 26:4588–4596. [PubMed: 17932491]

Van Nhieu GT, Ben-Ze'ev A, Sansonetti PJ. Modulation of bacterial entry into epithelial cells by association between vinculin and the Shigella IpaA invasin. EMBO J. 1997; 16:2717–2729. [PubMed: 9184218]

Wu YI, Frey D, Lungu OI, Jaehrig A, Schlichting I, Kuhlman B, Hahn KM. A genetically encoded photoactivatable Rac controls the motility of living cells. Nature. 2009; 461:104–108. [PubMed: 19693014]

Yao X, Rosen MK, Gardner KH. Estimation of the available free energy in a LOV2-Jα photoswitch. Nat. Chem. Biol. 2008; 4:491–497. [PubMed: 18604202]

Yazawa M, Sadaghiani AM, Hsueh B, Dolmetsch RE. Induction of protein-protein interactions in live cells using light. Nat. Biotechnol. 2009; 27:941–945. [PubMed: 19801976]

Young DD, Deiters A. Photochemical control of biological processes. Org. Biomol. Chem. 2007; 5:999–1005. [PubMed: 17377650]

Zoltowski BD, Vaccaro B, Crane BR. Mechanism-based tuning of a LOV domain photoreceptor. Nat. Chem. Biol. 2009; 5:827–834. [PubMed: 19718042]

Highlights

- The AsLOV2 domain can be used as a tool to photocontrol the peptides ipaA and SsrA
- LOV-ipaA and LOV-SsrA bind their effectors with 49-fold and 8-fold enhanced affinity in the light, respectively.
- Mutations that increase the difference between dark and lit state effector binding in both photoswitches are described.
- LOV-SsrA and LOV-ipaA are tuned by varying the location where the caged peptide sequences are embedded in the AsLOV2 Jα helix as well as varying the intrinsic affinity of the peptides for their targets.
- LOV-ipaA is applied to photocactivate gene transcription in *S. cerevisia*

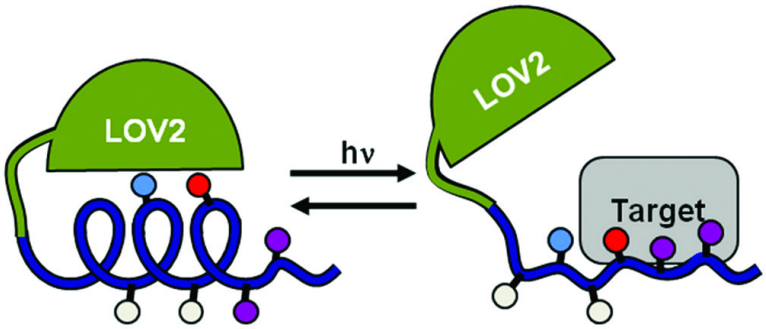

Figure 1. General design strategy for caging peptides using the AsLOV2 domain

Photoswitches are designed as sequence chimeras between the AsLOV2 Jα helix and the peptide to be caged. Residues that are important to AsLOV2-Jα interactions (cyan), important to peptide-target interaction (purple), important to both interactions (red), and residues that are important to neither interaction (white) are identified and mutated accordingly. Irradiation unfolds the Jα helix, and the peptide can bind its target.

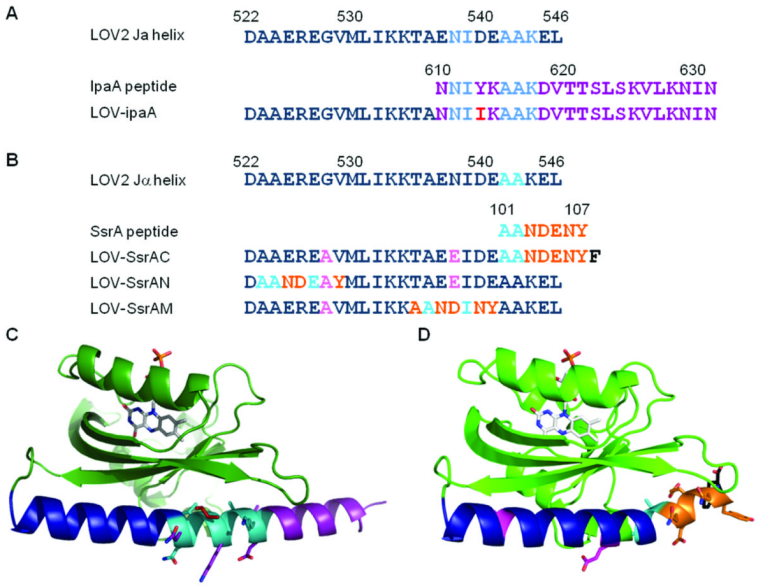

Figure 2. Design of LOV-ipaA and LOV-SsrA peptide photoswitches

(A) Sequence alignment of AsLOV2-Joc, ipaA, and LOV-ipaA. Jα sequence (blue) ipaA sequence (purple), chimera sequence (cyan), and designed residues (red) are indicated. (B) Sequence alignment of AsLOV2-Jα helix, SsrA peptide, and 3 LOV-SsrA designs, LOV-SsrAC, LOV-SsrAN, and LOV-SsrAM. Jα helix sequence (blue), SsrA sequence (orange), chimera sequence (cyan), designed positions (black), and helix stabilizing mutations (pink) are indicated. (C) Model of LOV-ipaA with residues colored as in (A). Residues N538, I539, A542, A543 K544 (cyan) as well as residues N537, K541, D545, V546 (purple) and I540 (red) are shown as sticks. (D) Model of LOV-SsrAC with residues colored as in (B). Residues A528,E538 (pink) as well as residues A542, A543 (cyan) and N544, D545, E546, N547, Y548 (orange) are shown as sticks. See also Figure S1.

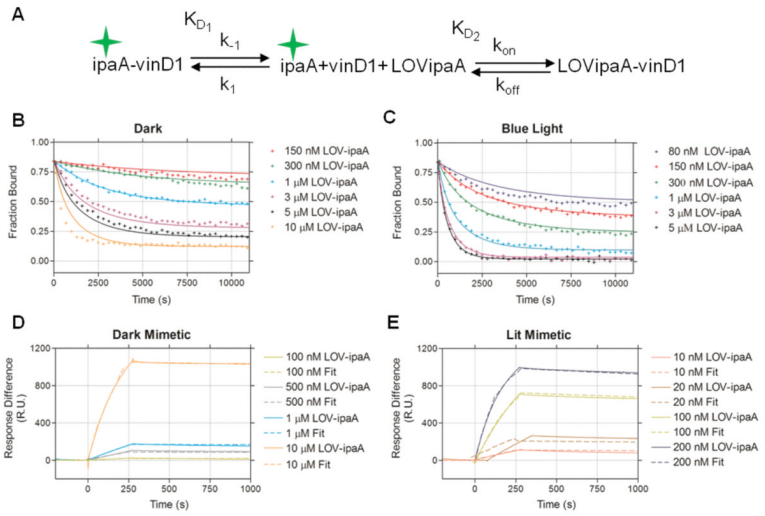

Figure 3. Measurement of rates and affinities of LOV-ipaA binding to vinculin

(A) Schematic of fluorescence polarization competition assay is shown. TAMRA labeled ipaA (ipaA*) is bound to vinculinD1 subdomain (vinD1). Vinculin dissociates from the complex with rates k_1, k_1 and binding affinity K_{D1}. LOV-ipaA (LOVipaA) binds vinculin with rates k_{on}, k_{off} and affinity K_{D2}. Fluorescence polarization decreases as the fraction of TAMRA-ipaA bound to vinculin decreases. (B) Fraction of TAMRA-ipaA bound to vinculin over time with varying concentrations of LOV-ipaA titrated in the dark and (C) under blue light. (D) Surface plasmon resonance measurements and first-order binding fit of LOV-ipaA L514K L531E C450A pseudo-dark and (E) LOV-ipaA L514K L531E A532E I53E pseudo-lit mutants. See also Figure S2.

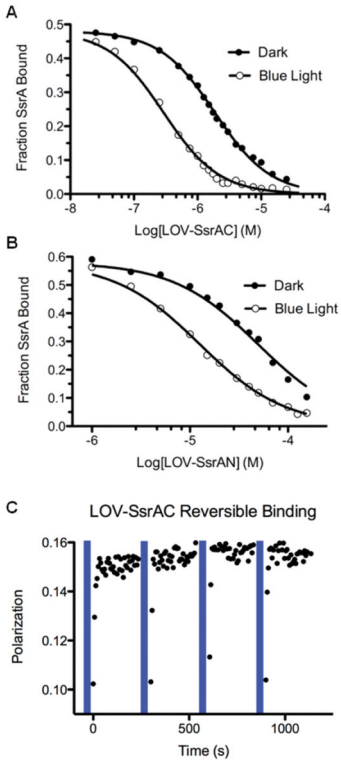

Figure 4. Competitve binding of LOV-SsrA to SspB in blue light and in darkness

Competitive binding assay of LOV-SsrAC (A) or LOV-SsrAN (B) to an equilibrium solution of SspB and 5(6)TAMRA-SsrA. 5(6)TAMRA-SsrA becomes unbound as LOV-SsrA competes for SspB binding. Binding to SspB was measured immediately after illumination with blue light (open circles) and after return to dark state (closed circles). (C) Reversible binding of LOV-SsrAC to SspB. A single titration point from the fluorescence polarization competition assay was repeatedly irradiated with blue light (blue bar = 60 seconds) and reversion to dark state equilibrium was monitored by polarization. See also Figure S3 and Table S1.

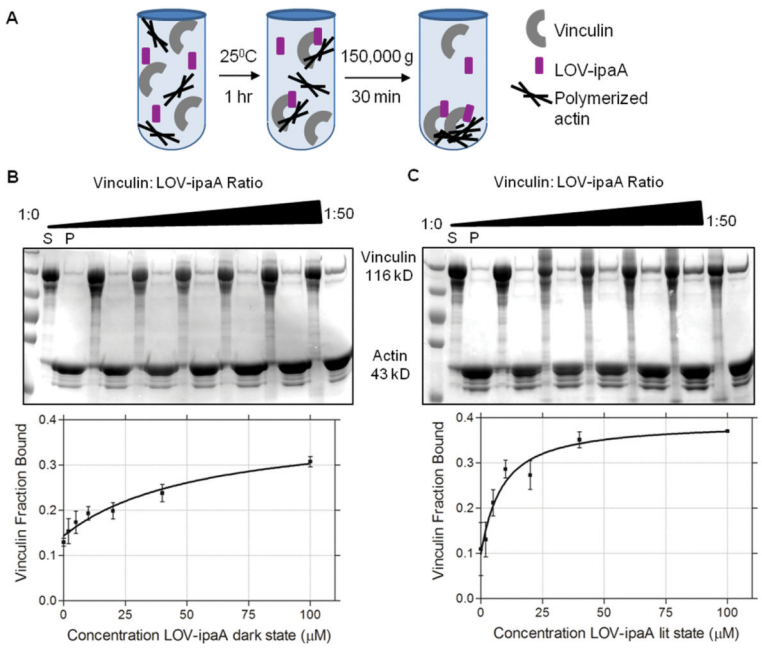

Figure 5. Binding of LOV-ipaA to full-length vinculin is measured through an actin co-sedimentation assay

(A) Full-length vinculin, LOV-ipaA, and polymerized actin are incubated 1 hr at room temperature. Vinculin that is bound to LOV-ipaA will bind polymerized actin. The mixture is centrifuged at 150,000 g, pelleting polymerized actin and all vinculin bound to it out of solution. (B) SDS-page gel of LOV-ipaA C450A and (C) LOV-ipaA A532E I536E actin co-sedimentation assay with vinculin. Molar ratios from 1:0 to 1:50 vinculin:LOV-ipaA were used. Supernatant (S) and pellet (P) fractions are shown side by side. Apparent binding affinity curves of fraction of vinculin bound to actin v. concentration of LOV-ipaA are plotted below. See also Table S2.

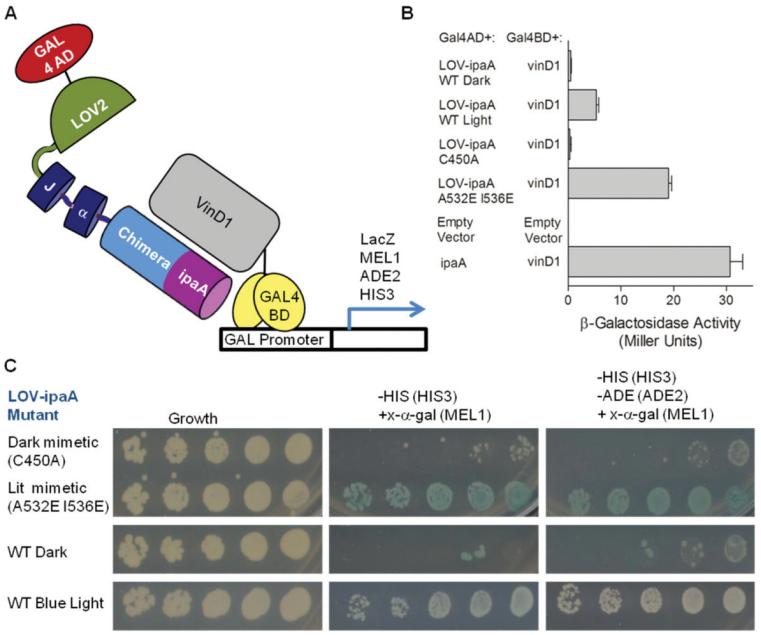

Figure 6. LOV-ipaA is used as a light-inducible heterodimerization tool

(A) LOV-ipaA L623A is linked to the GAL4 activation domain (AD), while vinculinD1 (vinD1) is linked to GAL4 binding domain (BD). Irradiation with blue light brings AD-LOV-ipaA into proximity to BD-vinD1, allowing for GAL-induced transcription of reporter genes LacZ, MEL1, HIS2, and ADE2. (B) LacZ transcription is quantified. β-galactosidase activity of *S. cerevisiae* mated strains containing BD and AD linked proteins, as specified, is shown. (C) *S. cerevisiae* mated strains containing BD-vinD1 and AD-LOV-ipaA mutants, as indicated, are grown in dark or blue light conditions on SD plates. Difference in levels of transcription of MEL1, HIS3 and ADE2 in dark v. lit state conditions is seen. See also Figure S4.

Table 1

Kinetic rates of LOV-ipaA binding vinculinD1

LOV-ipaA construct	k_{on} (M^{-1} s^{-1})	k_{off} (s^{-1})	K_D (nM)
Dark Mimetic (C450A)	$1.3 \pm 0.3 \times 10^{3}$	$8.0 \pm 0.7 \times 10^{-5}$	64 ± 9.5
WT Dark	$1.4 \pm 0.1 \times 10^{3}$	$9.6 \pm 0.1 \times 10^{-5}$	69 ± 0.5
Lit Mimetic (A532E I536E)	$2.9 \pm 2.0 \times 10^{4}$	$8.5 \pm 0.3 \times 10^{-5}$	3.0 ± 1.0
WT Blue Light	$1.3 \pm 0.3 \times 10^{4}$	$4.5 \pm 1.2 \times 10^{-5}$	3.5 ± 0.5
L514K L531E Dark	$4.5 \pm 1.5 \times 10^{2}$	$1.1 \pm 0.4 \times 10^{-4}$	245 ±5.0
L514K L531E Blue Light	$2.5 \pm 0.1 \times 10^{3}$	$1.3 \pm 0.1 \times 10^{-5}$	5.0 ± 0.1
G528A N538E Dark	$1.8 \pm 0.3 \times 10^{2}$	$8.2 \pm 0.2 \times 10^{-5}$	475 ± 75
G528A N538E Blue Light	$8.0 \pm 2.0 \times 10^{2}$	$1.2 \pm 0.1 \times 10^{-4}$	160 ± 40